SCIENCE CHINA
Information Sciences

• RESEARCH PAPER •

August 2021, Vol. 64 182310:1–182310:13
https://doi.org/10.1007/s11432-020-2935-6

Full-duplex two-way AF relaying systems with imperfect interference cancellation in Nakagami-m fading channels

Jianping TONG[1] & Caijun ZHONG[2*]

[1]*College of Science, Zhejiang University of Technology, Hangzhou* 310023*, China;*
[2]*Department of Information and Communication Engineering, Zhejiang University, Hangzhou* 310027*, China*

Received 31 January 2020/Revised 28 March 2020/Accepted 27 May 2020/Published online 2 June 2021

Abstract Full-duplex (FD) two-way relaying has the potential to substantially improve the spectral efficiency of the system, and is regarded as an enabling technology for the next generation wireless communication systems. Nevertheless, the joint effect of residual interference and channel fading condition on the fundamental performance of FD two-way relaying systems remains unclear. Motivated by this, this study considers a general FD two-way amplify-and-forward (AF) relaying system with imperfect interference cancellation in the versatile Nakagami-m fading channels, and presents a detailed analytical investigation on the outage performance of the system. The findings of the paper suggest that the performance of the FD two-way AF relaying system depends heavily on the residual interference strength, fading condition parameter m, and signal-to-noise ratio (SNR). The FD scheme outperforms the half-duplex (HD) two-way relaying counterpart in the low and moderate SNR regime, while becomes inferior in the high SNR regime, owing to strong residual interference. Also, compared to the channel fading condition of the information transmission channels, the impact of the channel fading condition of the interference channel on the system performance is relatively insignificant. Moreover, it is desirable to deploy the FD scheme when the channel fading condition of the information transmission channels is good, since it can effectively alleviate the detrimental effect of residual interference.

Keywords full-duplex, two-way relaying, Nakagami-m fading, outage probability, sum throughput

Citation Tong J P, Zhong C J. Full-duplex two-way AF relaying systems with imperfect interference cancellation in Nakagami-m fading channels. Sci China Inf Sci, 2021, 64(8): 182310, https://doi.org/10.1007/s11432-020-2935-6

1 Introduction

Relaying technique, which use intermediate relay nodes to forward the information signal, has been proven to be an effective method to extend the coverage of communication systems and improve the communication reliability [1, 2]. As such, it has been received considerable research interests in the past decade. To fully exploit the potential benefits provided by the relay, the two-way relaying approach has been proposed in the literature. Specifically, capitalizing on the breakthrough of physical layer network coding, it was demonstrated that two-way relaying can substantially improve the throughput of the system [3].

Besides, with the advancement in self-interference cancellation [4–6], the full-duplex (FD) mechanism, which allows concurrent transmission and reception over the same frequency band, has recently emerged as a promising candidate to boost the spectral efficiency. Hence, an appealing prospect has been envisioned by incorporating the FD mechanism into two-way relaying systems. In [7, 8], the spectral efficiency of the FD two-way amplify-and-forward (AF) relaying system was studied. In [9, 10], taking into account imperfect channel state information, the outage performance of FD two-way AF relaying and decode-and-forward relaying systems was respectively investigated. In [11], the spectral-energy efficiency tradeoff of FD two-way AF relaying systems was characterized. Later on, a relay selection scheme was proposed

* Corresponding author (email: caijunzhong@zju.edu.cn)

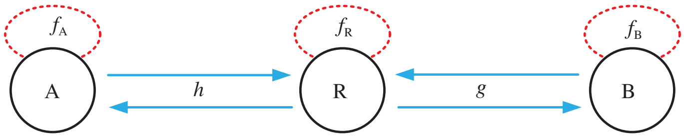

Figure 1 (Color online) System model, where the solid lines denote the information transmission channels, while the dash lines denote the loop back interference channels.

in [12], and antenna selection was considered in [13,14], while the outage performance of the user selection scheme was studied in [15]. In [16], power control was applied at the relay to improve the performance while reducing the relay power consumption.

The above contemporary list of references demonstrated significant progress in understanding the fundamental performance limits of FD two-way relaying systems. Nevertheless, a number of important questions remain to be addressed. In particular, to simplify the analytical treatment, most prior studies make the common assumption that part of the known interference can be perfectly removed, or that the residual interference is deterministic [8]. In addition, all the above studies consider the simple Rayleigh fading channels. Hence, the impact of channel fading condition on the system performance is largely unknown. Only in a recent study [17], the authors studied the outage performance of FD two-way AF relaying systems in the versatile Nakagami-m fading channels, by adopting the ideal assumption that perfect self-interference cancellation can be realized.

Motivated by the above key observations, this study considers the realistic scenario with imperfect known interference cancellation in the general Nakagami-m fading channels, and presents a detailed performance analysis on the outage probability of the system. In addition, to make a comparative study of the FD two-way relaying system, the corresponding half-duplex (HD) two-way relaying system is also studied. The main contribution of the study can be summarized as follows.

- General FD and HD two-way relaying system models with realistic interference cancellation capability are proposed.
- Closed-form expressions are derived for the outage probability lower bounds of both FD and HD two-way relaying systems, which involve only elementary functions, thereby providing efficient means for the evaluation of the system performance.
- At the high signal-to-noise ratio (SNR) regime, simplified asymptotical expressions are obtained. It is shown that the outage probability settles in the high SNR regime, owing to the severe residual interference.
- The outcomes of the study suggest that the performance of the FD two-way relaying system hinges on several mutually coupled factors, namely, fading parameter m, interference cancellation ability, and SNR. In general, FD outperforms HD in the low and moderates SNR regime, but becomes inferior in the high SNR regime, especially if the residual interference is strong. In addition, it is desirable to deploy the FD scheme in a less severe fading environment, where the detrimental effect of residual interference can be better mitigated.

The remainder of the paper is organized as follows. Section 2 introduces the FD two-way relaying system model. Section 3 presents a detailed performance analysis of the FD two-way relaying systems. Section 4 deals with the corresponding HD two-way relaying system. Numerical simulation results are presented in Section 5. Finally, Section 6 concludes the paper.

2 System model

Let us consider a communication system consisting of two nodes A and B communicating with each other with the assistance of an intermediate relay node R, as illustrated in Figure 1 [18, 19][1]. The relay node operates in the full-duplex mode and adopts the AF relaying protocol. We consider the quasi-static block fading channels, and assume the channel reciprocity holds as in [7, 8, 12].

As such, the received signal at the relay is given by

$$y_{\mathrm{R}}[i] = hx_{\mathrm{A}}[i] + gx_{\mathrm{B}}[i] + f_{\mathrm{R}}x_{\mathrm{R}}[i] + n_{\mathrm{R}}[i], \tag{1}$$

1) The considered model is also applicable for UAV relaying systems [18, 19], as long as the UAVs are FD compatible.

where $x_{\mathrm{A}}[i]$ and $x_{\mathrm{B}}[i]$ are the desired information symbols from A and B at the i-th time slot satisfying $\mathrm{E}\{|x_{\mathrm{A}}[i]|^2\} = P_{\mathrm{A}}$ and $\mathrm{E}\{|x_{\mathrm{B}}[i]|^2\} = P_{\mathrm{B}}$, respectively, while $x_{\mathrm{R}}[i]$ with $\mathrm{E}\{|x_{\mathrm{R}}[i]|^2\} = P_{\mathrm{R}}$ is the relay loop back interference owing to full duplex operation. The complex scalers h and g denote the channel coefficients between A and R, B and R, respectively, while f_{R} denotes the self-interference channel coefficient at the relay. The term $n_{\mathrm{R}}[i]$ is the additive white Gaussian noise modeled as $n_{\mathrm{R}}[i] \sim CN(0, N_0)$.

Since the relay node knows the transmitted symbol $x_{\mathrm{R}}[i]$, interference cancellation methods can be applied to eliminate the loop back interference $f_{\mathrm{R}}x_{\mathrm{R}}[i]$[2)]. Nevertheless, because of imperfect channel state information and various non-ideal factors, complete elimination of the loop back interference is difficult in practice. Therefore, residual self-interference is expected to exist, which is defined as $\hat{f}_{\mathrm{R}}\hat{x}_{\mathrm{R}}[i]$, where $\hat{x}_{\mathrm{R}}[i]$ is the residual interference with $\mathrm{E}\{|\hat{x}_{\mathrm{R}}[i]|^2\} = \kappa_1^2 P_{\mathrm{R}}$, $0 \leqslant \kappa_1 \leqslant 1$ is a constant depending on the effectiveness of the interference cancellation schemes, $\hat{f}_{\mathrm{R}}$ models the post-cancellation channel coefficient [20]. Hence, after loop back interference cancellation, the signal at the relay $\hat{y}_{\mathrm{R}}[i]$ can be expressed as

$$\hat{y}_{\mathrm{R}}[i] = hx_{\mathrm{A}}[i] + gx_{\mathrm{B}}[i] + \hat{f}_{\mathrm{R}}\hat{x}_{\mathrm{R}}[i] + n_{\mathrm{R}}[i]. \tag{2}$$

With AF protocol, the transmit signal at the relay $x_{\mathrm{R}}[i]$ appeared in (1) is a scaled version of the time delayed received signal after interference cancellation, which can be expressed as

$$x_{\mathrm{R}}[i] = \alpha_1 \hat{y}_{\mathrm{R}}[i - \tau], \tag{3}$$

where α_1 is the relay amplification factor given by

$$\alpha_1^2 = \frac{P_{\mathrm{R}}}{|h|^2 P_{\mathrm{A}} + |g|^2 P_{\mathrm{B}} + |\hat{f}_R|^2 \kappa_1^2 P_{\mathrm{R}} + N_0}. \tag{4}$$

Therefore, the signals received at nodes A and B are given by

$$y_{\mathrm{A}}[i] = hx_{\mathrm{R}}[i] + f_{\mathrm{A}}x_{\mathrm{A}}[i] + n_{\mathrm{A}}[i] \text{ and} \tag{5}$$

$$y_{\mathrm{B}}[i] = gx_{\mathrm{R}}[i] + f_{\mathrm{B}}x_{\mathrm{B}}[i] + n_{\mathrm{B}}[i], \tag{6}$$

respectively. Similarly, $f_{\mathrm{A}}x_{\mathrm{A}}[i]$ and $f_{\mathrm{B}}x_{\mathrm{B}}[i]$ are the loop back interference at nodes A and B, while f_{A} and f_{B} are the loop back interference channel of nodes A and B, respectively. The terms $n_{\mathrm{A}}[i]$ and $n_{\mathrm{B}}[i]$ are the AWGN modeled as $n_{\mathrm{A}}[i] \sim CN(0, N_0)$ and $n_{\mathrm{B}}[i] \sim CN(0, N_0)$, respectively.

Without loss of generality, we focus on the analysis of node A. Substituting $x_{\mathrm{R}}[i]$ given in (3) into (5), we have

$$y_{\mathrm{A}}[i] = h^2\alpha_1 x_{\mathrm{A}}[i-\tau] + h\alpha_1 g x_{\mathrm{B}}[i-\tau] + h\alpha_1 \hat{f}_{\mathrm{R}}\hat{x}_{\mathrm{R}}[i-\tau] + h\alpha_1 n_{\mathrm{R}}[i-\tau] + f_{\mathrm{A}}x_{\mathrm{A}}[i] + n_{\mathrm{A}}[i]. \tag{7}$$

For node A, the desired information symbol is $x_{\mathrm{B}}[i-\tau]$, while $h^2\alpha_1 x_{\mathrm{A}}[i-\tau]$ is the self-interference and $f_{\mathrm{A}}x_{\mathrm{A}}[i]$ is the loop back interference[3)]. Since node A is aware of $x_{\mathrm{A}}[i-\tau]$ and $x_{\mathrm{A}}[i]$, it can also apply various interference cancellation methods to remove the self-interference and loop back interference. In most prior studies, it is often assumed that the self-interference is perfectly cancelled. In contrast, we consider the more practical scenario with residual self-interference. In particular, the signal after interference mitigation is expressed as

$$\hat{y}_{\mathrm{A}}[i] = h\alpha_1 g x_{\mathrm{B}}[i-\tau] + h\alpha_1 \hat{f}_{\mathrm{R}}\hat{x}_{\mathrm{R}}[i-\tau] + h\alpha_1 n_{\mathrm{R}}[i-\tau] + \hat{f}_{\mathrm{A}}\hat{x}_{\mathrm{A}}[i] + \hat{h}_{\mathrm{A}}\hat{x}_{\mathrm{A}}[i-\tau] + n_{\mathrm{A}}[i], \tag{8}$$

where $\hat{x}_{\mathrm{A}}[i]$ and $\hat{x}_{\mathrm{A}}[i-\tau]$ are the residual loop back interference and residual self-interference with $\mathrm{E}\{|\hat{x}_{\mathrm{A}}[i]|^2\} = \kappa_2^2 P_{\mathrm{A}}$ and $\mathrm{E}\{|\hat{x}_{\mathrm{A}}[i-\tau]|^2\} = \kappa_3^2 P_{\mathrm{A}}$, respectively. Also, $0 \leqslant \kappa_2 \leqslant 1$ and $0 \leqslant \kappa_3 \leqslant 1$ are constants depending on the effectiveness of the interference cancellation schemes, and $\hat{f}_{\mathrm{R}}$ and $\hat{h}_{\mathrm{A}}$ model the post-cancellation channel coefficients.

2) We consider instant detection where individual symbols are separately processed, as such, signals from the prior time slots are treated as interference.

3) Please note, we distinguish two different types of interference depending on the signal prorogation path, and the term "self-interference" is used for the interference from the relay, while the term "loop back interference" is used for the interference from the own transmitter.

Therefore, the end-to-end signal to interference and noise ratio (SINR) at node A is given by

$$\gamma_{\rm A} = \frac{\alpha_1^2|h|^2|g|^2P_{\rm B}}{\alpha_1^2|h|^2|\hat{f}_{\rm R}|^2\kappa_1^2P_{\rm R} + \alpha_1^2|h|^2N_0 + |\hat{f}_{\rm A}|^2\kappa_2^2P_{\rm A} + |\hat{h}_{\rm A}|^2\kappa_3^2P_{\rm A} + N_0} \tag{9}$$

$$= \frac{\frac{\rho_{\rm A}|h|^2P_{\rm A}}{|\hat{f}_{\rm A}|^2\kappa_2^2P_{\rm A}+|\hat{h}_{\rm A}|^2\kappa_3^2P_{\rm A}+N_0}\frac{|g|^2P_{\rm B}}{|\hat{f}_{\rm R}|^2\kappa_1^2P_{\rm R}+N_0}}{\frac{\rho_{\rm A}|h|^2P_{\rm A}}{|\hat{f}_{\rm A}|^2\kappa_2^2P_{\rm A}+|\hat{h}_{\rm A}|^2\kappa_3^2P_{\rm A}+N_0} + \frac{|h|^2P_{\rm A}+|g|^2P_{\rm B}}{|\hat{f}_R|^2\kappa_1^2P_{\rm R}+N_0} + 1}, \tag{10}$$

where $\rho_{\rm A} = \frac{P_{\rm R}}{P_{\rm A}}$.

Following the same analysis, the end-to-end SINR at node B can be obtained as

$$\gamma_{\rm B} = \frac{\frac{\rho_{\rm B}|g|^2P_{\rm B}}{|\hat{f}_{\rm B}|^2\kappa_4^2P_{\rm B}+|\hat{h}_{\rm B}|^2\kappa_5^2P_{\rm B}+N_0}\frac{|h|^2P_{\rm A}}{|\hat{f}_R|^2\kappa_1^2P_{\rm R}+N_0}}{\frac{\rho_{\rm B}|g|^2|P_{\rm B}}{|\hat{f}_{\rm B}|^2\kappa_4^2P_{\rm B}+|\hat{h}_{\rm B}|^2\kappa_5^2P_{\rm B}+N_0} + \frac{|h|^2P_{\rm A}+|g|^2P_{\rm B}}{|\hat{f}_R|^2\kappa_1^2P_{\rm R}+N_0} + 1}, \tag{11}$$

where $\rho_{\rm B} = \frac{P_{\rm R}}{P_{\rm B}}$, $\hat{f}_{\rm B}$ and $\hat{h}_{\rm B}$ are the post-cancellation channel coefficients for the loop back interference and self-interference, respectively. Also, $0 \leqslant \kappa_4 \leqslant 1$ and $0 \leqslant \kappa_5 \leqslant 1$ are constant parameters denoting the effectiveness of the interference cancellation schemes.

In the current paper, we consider the general Nakagami-m fading. Hence, all the channel gains are Gamma distributed. Let $\text{Gamma}(\alpha, \beta)$ denote the Gamma distribution with shape parameter α and scale parameter β, and then, $|h|^2 \sim \text{Gamma}(m_1, \frac{\Omega_1}{m_1})$, $|g|^2 \sim \text{Gamma}(m_2, \frac{\Omega_2}{m_2})$, $|\hat{f}_{\rm A}|^2 \sim \text{Gamma}(m_3, \frac{\Omega_3}{m_3})$, $|\hat{h}_{\rm A}|^2 \sim \text{Gamma}(m_4, \frac{\Omega_4}{m_4})$, $|\hat{f}_{\rm R}|^2 \sim \text{Gamma}(m_5, \frac{\Omega_5}{m_5})$, $|\hat{f}_{\rm B}|^2 \sim \text{Gamma}(m_6, \frac{\Omega_6}{m_6})$, $|\hat{h}_{\rm B}|^2 \sim \text{Gamma}(m_7, \frac{\Omega_7}{m_7})$. Also, the cumulative distribution functions (c.d.f.) and probability distribution functions (p.d.f.) of the channel gains are given by

$$F(x) = 1 - \sum_{j=0}^{m_i-1} \frac{1}{j!}\left(\frac{m_i x}{\Omega_i}\right)^j \mathrm{e}^{-\frac{m_i x}{\Omega_i}}, \quad x \geqslant 0, \tag{12}$$

$$f(x) = \frac{m_i^{m_i}}{\Gamma(m_i)\Omega_i^{m_i}} x^{m_i-1}\mathrm{e}^{-\frac{m_i x}{\Omega_i}}, \quad x \geqslant 0, \tag{13}$$

for $i = 1, \ldots, 7$.

For notational convenience, let $\gamma_1 = \frac{|h|^2P_{\rm A}}{N_0}$, $\gamma_2 = \frac{|g|^2P_{\rm B}}{N_0}$, $\gamma_3 = \frac{|\hat{f}_{\rm A}|^2\kappa_2^2P_{\rm A}}{N_0} + \frac{|\hat{h}_{\rm A}|^2\kappa_3^2P_{\rm A}}{N_0} + 1$, $\gamma_4 = \frac{|\hat{f}_{\rm R}|^2\kappa_1^2P_{\rm R}}{N_0} + 1$ and $\gamma_5 = \frac{|\hat{f}_{\rm B}|^2\kappa_4^2P_{\rm B}}{N_0} + \frac{|\hat{h}_{\rm B}|^2\kappa_5^2P_{\rm B}}{N_0} + 1$. Then, the end-to-end SINRs at nodes A and B can be expressed as

$$\gamma_{\rm A} = \frac{\frac{\rho_{\rm A}\gamma_1}{\gamma_3}\frac{\gamma_2}{\gamma_4}}{\frac{\rho_{\rm A}\gamma_1}{\gamma_3} + \frac{\gamma_1+\gamma_2}{\gamma_4} + 1} \tag{14}$$

and

$$\gamma_{\rm B} = \frac{\frac{\rho_{\rm B}\gamma_2}{\gamma_5}\frac{\gamma_1}{\gamma_4}}{\frac{\rho_{\rm B}\gamma_2}{\gamma_5} + \frac{\gamma_1+\gamma_2}{\gamma_4} + 1}, \tag{15}$$

respectively.

3 Performance analysis

In this section, we present a detailed performance analysis of the proposed FD two-way relaying systems in terms of outage probability and effective sum throughput. Let us assume that the nodes A and B are transmitting at constant rates $R_{\rm A}^{\rm FD}$ and $R_{\rm B}^{\rm FD}$, respectively. Also, let $\theta_{\rm A} = 2^{R_{\rm B}^{\rm FD}} - 1$ and $\theta_{\rm B} = 2^{R_{\rm A}^{\rm FD}} - 1$, and then the outage probability, defined as the probability of instantaneous SINR falls below a predefined threshold, at nodes A and B can be expressed as

$$P_{\rm OA}^{\rm F} = \Pr(\gamma_{\rm A} < \theta_{\rm A}) \ \text{ and } \ P_{\rm OB}^{\rm F} = \Pr(\gamma_{\rm B} < \theta_{\rm B}), \tag{16}$$

respectively. In addition, the effective sum throughput can be computed by

$$\tau_{\rm FD} = R_{\rm B}(1 - P_{\rm OA}^{\rm F}) + R_{\rm A}(1 - P_{\rm OB}^{\rm F}). \tag{17}$$

3.1 Outage probability

Owing to the the complicated SINR expressions given in (14) and (15), an exact analytical characterization of the outage probability is difficult. Hence, in the following, we focus on deriving tight outage lower bounds for the outage probability.

To start with, we present upper bounds of the end-to-end SINR $\gamma_{\rm A}$ and $\gamma_{\rm B}$.

Corollary 1. The end-to-end SINR $\gamma_{\rm A}$ and $\gamma_{\rm B}$ can be upper bounded by

$$\gamma_{\rm A} \leqslant \gamma_{\rm A}^{\rm up} = \rho_{\rm A} \min\left(\frac{\gamma_2}{\gamma_3+\rho_{\rm A}\gamma_4}, \frac{\gamma_1}{\gamma_3}\right) \tag{18}$$

and

$$\gamma_{\rm B} \leqslant \gamma_{\rm B}^{\rm up} = \rho_{\rm B} \min\left(\frac{\gamma_1}{\gamma_5+\rho_{\rm B}\gamma_4}, \frac{\gamma_2}{\gamma_5}\right), \tag{19}$$

respectively.

Proof. Without loss of generality, we focus on $\gamma_{\rm A}$. From (14), it is easy to see that

$$\gamma_{\rm A} \leqslant \frac{\frac{\rho_{\rm A}\gamma_1}{\gamma_3}\frac{\gamma_2}{\gamma_4}}{\frac{\rho_{\rm A}\gamma_1}{\gamma_3}+\frac{\gamma_1+\gamma_2}{\gamma_4}}. \tag{20}$$

With some simple algebraic manipulation, we have

$$\gamma_{\rm A} \leqslant \frac{\rho_{\rm A}\gamma_1\gamma_2}{(\rho_{\rm A}\gamma_4+\gamma_3)\gamma_1+\gamma_3\gamma_2} = \rho_{\rm A}\frac{\frac{\gamma_1}{\gamma_3}\frac{\gamma_2}{\rho_{\rm A}\gamma_4+\gamma_3}}{\frac{\gamma_1}{\gamma_3}+\frac{\gamma_2}{\rho_{\rm A}\gamma_4+\gamma_3}}. \tag{21}$$

To this end, invoking the well-known inequality $\frac{xy}{x+y} \leqslant \min(x,y)$ yields the desired result.

Capitalizing on the above SINR upper bound, we now derive a lower bound for the outage probability. Specifically, we have the following key result.

Theorem 1. The outage probability lower bounds at node A $P_{\rm OA}^{\rm FL}$ and node B $P_{\rm OB}^{\rm FL}$ are given by

$$\begin{aligned} P_{\rm OA}^{\rm F} \geqslant & P_{\rm OA}^{\rm FL} = 1-\beta_3^{m_3}\beta_4^{m_4}\beta_5^{m_5}{\rm e}^{-\frac{\beta_1\theta_{\rm A}+\beta_2\theta_{\rm A}}{\rho_{\rm A}}-\beta_2\theta_{\rm A}} \\ & \times \sum_{i=0}^{m_1-1}\frac{1}{i!}\left(\frac{\beta_1\theta_{\rm A}}{\rho_{\rm A}}\right)^i \sum_{j=0}^{m_2-1}\frac{1}{j!}\left(\frac{\beta_2\theta_{\rm A}}{\rho_{\rm A}}\right)^j \sum_{k=0}^{j}\binom{j}{k}\frac{\rho_{\rm A}^{j-k}}{\Gamma(m_5)}\sum_{p=0}^{j-k}\binom{j-k}{p}\frac{\Gamma(m_5+p)}{(\beta_5+\beta_2\theta_{\rm A})^{m_5+p}} \\ & \times \left(\sum_{s=1}^{m_3}\frac{\prod_{j=1}^{s-1}(1-m_4-j)\,(\beta_4-\beta_3)^{1-m_4-s}}{(m_3-s)!(s-1)!}\sum_{t=0}^{k+i}\binom{k+i}{t}\left(\beta_3+\frac{\beta_1\theta_{\rm A}+\beta_2\theta_{\rm A}}{\rho_{\rm A}}\right)^{-z_1(3)}\Gamma(z_1(3))\right. \\ & \left. +\sum_{s=1}^{m_4}\frac{\prod_{j=1}^{s-1}(1-m_3-j)\,(\beta_3-\beta_4)^{1-m_3-s}}{(m_4-s)!(s-1)!}\sum_{t=0}^{k+i}\binom{k+i}{t}\left(\beta_4+\frac{\beta_1\theta_{\rm A}+\beta_2\theta_{\rm A}}{\rho_{\rm A}}\right)^{-z_1(4)}\Gamma(z_1(4))\right) \end{aligned}$$

and

$$\begin{aligned} P_{\rm OB}^{\rm F} \geqslant & P_{\rm OB}^{\rm FL} = 1-\beta_5^{m_5}\beta_6^{m_6}\beta_7^{m_7}{\rm e}^{-\frac{\beta_1\theta_{\rm B}+\beta_2\theta_{\rm B}}{\rho_{\rm B}}-\beta_1\theta_{\rm B}} \\ & \times \sum_{i=0}^{m_1-1}\frac{1}{i!}\left(\frac{\beta_1\theta_{\rm B}}{\rho_{\rm B}}\right)^i \sum_{j=0}^{m_2-1}\frac{1}{j!}\left(\frac{\beta_2\theta_{\rm B}}{\rho_{\rm B}}\right)^j \sum_{k=0}^{i}\binom{i}{k}\frac{\rho_{\rm B}^{i-k}}{\Gamma(m_5)}\sum_{p=0}^{i-k}\binom{i-k}{p}\frac{\Gamma(m_5+p)}{(\beta_5+\beta_1\theta_{\rm B})^{m_5+p}} \\ & \times \left(\sum_{s=1}^{m_6}\frac{\prod_{j=1}^{s-1}(1-m_7-j)\,(\beta_7-\beta_6)^{1-m_7-s}}{(m_6-s)!(s-1)!}\sum_{t=0}^{k+j}\binom{k+j}{t}\left(\beta_6+\frac{\beta_1\theta_{\rm B}+\beta_2\theta_{\rm B}}{\rho_{\rm B}}\right)^{-z_1(6)}\Gamma(z_1(6))\right. \\ & \left. +\sum_{s=1}^{m_7}\frac{\prod_{j=1}^{s-1}(1-m_6-j)\,(\beta_6-\beta_7)^{1-m_6-s}}{(m_7-s)!(s-1)!}\sum_{t=0}^{k+j}\binom{k+j}{t}\left(\beta_7+\frac{\beta_1\theta_{\rm B}+\beta_2\theta_{\rm B}}{\rho_{\rm B}}\right)^{-z_1(7)}\Gamma(z_1(7))\right), \end{aligned}$$

respectively, where $z_1(q) \triangleq m_q+t-s+1$ for $q=3,4,6,7$, $\beta_1 = \frac{m_1 N_0}{\Omega_1 P_{\rm A}}$, $\beta_2 = \frac{m_2 N_0}{\Omega_2 P_{\rm B}}$, $\beta_3 = \frac{m_3 N_0}{\Omega_3 \kappa_2^2 P_{\rm A}}$, $\beta_4 = \frac{m_4 N_0}{\Omega_4 \kappa_3^2 P_{\rm A}}$, $\beta_5 = \frac{m_5 N_0}{\Omega_5 \kappa_1^2 P_{\rm R}}$, $\beta_6 = \frac{m_6 N_0}{\Omega_6 \kappa_4^2 P_{\rm B}}$, and $\beta_7 = \frac{m_7 N_0}{\Omega_7 \kappa_5^2 P_{\rm B}}$. Also, $\Gamma(x)$ is the Gamma function.

Proof. See Appendix A.

Theorem 1 presents a closed-form expression for the outage probability, which is valid for arbitrary configurations. In addition, it only involves elementary functions, hence it provides an efficient means to evaluate the outage performance.

For the special case with Rayleigh fading, simplified expressions are available as shown in the following corollary.

Corollary 2. For Rayleigh fading channels, the outage probability lower bounds at node A $P_{\rm OA}^{L}$ and node B $P_{\rm OA}^{L}$ reduce to

$$P_{\rm OA}^{\rm FL}=1-\frac{\beta_3\beta_4\beta_5}{\beta_4-\beta_3}\frac{{\rm e}^{-\frac{\beta_1\theta_{\rm A}+\beta_2\theta_{\rm A}}{\rho_{\rm A}}-\beta_2\theta_{\rm A}}}{\beta_2\theta_{\rm A}+\beta_5}\left(\frac{1}{\beta_3+\frac{\beta_1\theta_{\rm A}+\beta_2\theta_{\rm A}}{\rho_{\rm A}}}-\frac{1}{\beta_4+\frac{\beta_1\theta_{\rm A}+\beta_2\theta_{\rm A}}{\rho_{\rm A}}}\right) \tag{22}$$

and

$$P_{\rm OB}^{\rm FL}=1-\frac{\beta_5\beta_6\beta_7}{\beta_7-\beta_6}\frac{{\rm e}^{-\frac{\beta_1\theta_{\rm B}+\beta_2\theta_{\rm B}}{\rho_{\rm B}}-\beta_1\theta_{\rm B}}}{\beta_1\theta_{\rm B}+\beta_5}\left(\frac{1}{\beta_6+\frac{\beta_1\theta_{\rm B}+\beta_2\theta_{\rm B}}{\rho_{\rm B}}}-\frac{1}{\beta_7+\frac{\beta_1\theta_{\rm B}+\beta_2\theta_{\rm B}}{\rho_{\rm B}}}\right), \tag{23}$$

respectively.

Proof. The result can be obtained by setting $m_i=1$ in Theorem 1.

Given the outage lower bound, the effective sum throughput of the system can be upper bounded by

$$\tau_{\rm FD}\leqslant\tau_{\rm FD}^{\rm U}=R_{\rm B}^{\rm FD}(1-P_{\rm OA}^{\rm FL})+R_{\rm A}^{\rm FD}(1-P_{\rm OB}^{\rm FL}). \tag{24}$$

3.2 Asymptotic analysis

To gain further insights, we now look into the asymptotic large power regime. For two-way relaying systems, we are interested in the asymptotic regime, where the transmit powers at all three nodes become large, i.e., $P_{\rm A}\to\infty$, $P_{\rm B}=k_aP_{\rm A}$, and $P_{\rm R}=\rho_{\rm A}P_{\rm A}$. And we have the following key result.

Proposition 1. In the asymptotic high SNR regime, the outage probabilities at nodes A and B can be approximated by

$$\begin{aligned}P_{\rm OA}^{\rm FL}\approx\,&1-\left(\frac{m_3N_0}{\Omega_3\kappa_2^2}\right)^{m_3}\left(\frac{m_4N_0}{\Omega_4\kappa_3^2}\right)^{m_4}\left(\frac{m_5N_0}{\Omega_5\kappa_1^2\rho_{\rm A}}\right)^{m_5}\\&\times\sum_{i=0}^{m_1-1}\frac{1}{i!}\left(\frac{m_1N_0\theta_{\rm A}}{\Omega_1\rho_{\rm A}}\right)^i\sum_{j=0}^{m_2-1}\frac{1}{j!}\left(\frac{m_2N_0\theta_{\rm A}}{\Omega_2k_a\rho_{\rm A}}\right)^j\sum_{k=0}^{j}\binom{j}{k}\frac{\rho_{\rm A}^{j-k}}{\Gamma(m_5)}\frac{\Gamma(m_5+j-k)}{(\frac{m_5N_0}{\Omega_5\kappa_1^2\rho_{\rm A}}+\frac{m_2N_0\theta_{\rm A}}{\Omega_2k_a})^{m_5+j-k}}\\&\times\left(\sum_{s=1}^{m_3}\frac{\prod_{j=1}^{s-1}(1-m_4-j)(\frac{m_4N_0}{\Omega_4\kappa_3^2}-\frac{m_3N_0}{\Omega_3\kappa_2^2})^{1-m_4-s}}{(m_3-s)!(s-1)!}\left(\frac{m_3N_0}{\Omega_3\kappa_2^2}+\frac{m_1N_0\theta_{\rm A}}{\Omega_1\rho_{\rm A}}+\frac{m_2N_0\theta_{\rm A}}{\Omega_2k_a\rho_{\rm A}}\right)^{-z_2(3)}\Gamma(z_2(3))\right.\\&\left.+\sum_{s=1}^{m_4}\frac{\prod_{j=1}^{s-1}(1-m_3-j)(\frac{m_3N_0}{\Omega_3\kappa_2^2}-\frac{m_4N_0}{\Omega_4\kappa_3^2})^{1-m_3-s}}{(m_4-s)!(s-1)!}\left(\frac{m_4N_0}{\Omega_4\kappa_3^2}+\frac{m_1N_0\theta_{\rm A}}{\Omega_1\rho_{\rm A}}+\frac{m_2N_0\theta_{\rm A}}{\Omega_2k_a\rho_{\rm A}}\right)^{-z_2(4)}\Gamma(z_2(4))\right)\end{aligned} \tag{25}$$

and

$$\begin{aligned}P_{\rm OB}^{\rm FL}\approx\,&1-\left(\frac{m_5N_0}{\Omega_5\kappa_1^2\rho_{\rm B}}\right)^{m_5}\left(\frac{m_6N_0}{\Omega_6\kappa_4^2}\right)^{m_6}\left(\frac{m_7N_0}{\Omega_7\kappa_5^2}\right)^{m_7}\\&\times\sum_{i=0}^{m_1-1}\frac{1}{i!}\left(\frac{k_am_1N_0\theta_{\rm B}}{\Omega_1\rho_{\rm B}}\right)^i\sum_{j=0}^{m_2-1}\frac{1}{j!}\left(\frac{m_2N_0\theta_{\rm B}}{\Omega_2\rho_{\rm B}}\right)^j\sum_{k=0}^{i}\binom{i}{k}\frac{\rho_{\rm B}^{i-k}}{\Gamma(m_5)}\frac{\Gamma(m_5+i-k)}{(\frac{m_5N_0}{\Omega_5\kappa_1^2\rho_{\rm B}}+\frac{k_am_1N_0\theta_{\rm B}}{\Omega_1})^{m_5+i-k}}\\&\times\left(\sum_{s=1}^{m_6}\frac{\prod_{j=1}^{s-1}(1-m_7-j)(\frac{m_7N_0}{\Omega_7\kappa_5^2}-\frac{m_6N_0}{\Omega_6\kappa_4^2})^{1-m_7-s}}{(m_6-s)!(s-1)!}\left(\frac{m_6N_0}{\Omega_6\kappa_4^2}+\frac{k_am_1N_0\theta_{\rm B}}{\Omega_1\rho_{\rm B}}+\frac{m_2N_0\theta_{\rm B}}{\Omega_2\rho_{\rm B}}\right)^{-z_2(6)}\Gamma(z_2(6))\right.\end{aligned}$$

$$+\sum_{s=1}^{m_7}\frac{\prod_{j=1}^{s-1}(1-m_6-j)(\frac{m_6N_0}{\Omega_6\kappa_4^2}-\frac{m_7N_0}{\Omega_7\kappa_5^2})^{1-m_6-s}}{(m_7-s)!(s-1)!}\left(\frac{m_7N_0}{\Omega_7\kappa_5^2}+\frac{k_am_1N_0\theta_{\rm B}}{\Omega_1\rho_{\rm B}}+\frac{m_2N_0\theta_{\rm B}}{\Omega_2\rho_{\rm B}}\right)^{-z_2(7)}\Gamma(z_2(7))\Bigg), \tag{26}$$

where $z_2(q)\triangleq m_q+k+j-s+1$ for $q=3,4,6,7$.

Proof. The key idea is that at the high SNR regime, only the most significant terms matter. For instance, in $\sum_{t=0}^{k+i}\binom{k+i}{t}(\beta_3+\frac{\beta_1\theta_{\rm A}+\beta_2\theta_{\rm A}}{\rho_{\rm A}})^{-(m_3+t-s+1)}$, the $(t=k+i)$th item is the most significant term, and the other terms could be neglected. Then, the final expression can be obtained after some simple algebraic manipulations.

Proposition 1 suggests that, at the high SNR regime, the outage probabilities at both nodes A and B saturate, i.e., zero diversity order is achieved. This is in sharp contrast with the findings reported in literature, where it was proven that interference does not reduce the achievable diversity order. The reason is that prior studies mainly focus on the fixed interference power scenarios, while in the current work, the self-interference or loop back interference is proportionate to the transmit powers.

Corollary 3. For Rayleigh fading channels, the outage probabilities at nodes A and B can be approximated by

$$P_{\rm OA}^{\rm FL}\approx 1-\left(\frac{N_0}{\Omega_3\kappa_2^2}\right)\left(\frac{N_0}{\Omega_4\kappa_3^2}\right)\left(\frac{N_0}{\Omega_5\kappa_1^2\rho_{\rm A}}\right)\left(\frac{N_0}{\Omega_5\kappa_1^2\rho_{\rm A}}+\frac{N_0\theta_{\rm A}}{\Omega_2k_a}\right)^{-1}\left(\frac{N_0}{\Omega_4\kappa_3^2}-\frac{N_0}{\Omega_3\kappa_2^2}\right)^{-1}$$
$$\times\left(\left(\frac{N_0}{\Omega_3\kappa_2^2}+\frac{N_0\theta_{\rm A}}{\Omega_1\rho_{\rm A}}+\frac{N_0\theta_{\rm A}}{\Omega_2k_a\rho_{\rm A}}\right)^{-1}-\left(\frac{N_0}{\Omega_4\kappa_3^2}+\frac{N_0\theta_{\rm A}}{\Omega_1\rho_{\rm A}}+\frac{N_0\theta_{\rm A}}{\Omega_2k_a\rho_{\rm A}}\right)^{-1}\right), \tag{27}$$

and

$$P_{\rm OB}^{\rm FL}\approx 1-\left(\frac{N_0}{\Omega_5\kappa_1^2\rho_{\rm B}}\right)\left(\frac{N_0}{\Omega_6\kappa_4^2}\right)\left(\frac{N_0}{\Omega_7\kappa_5^2}\right)\left(\frac{N_0}{\Omega_5\kappa_1^2\rho_{\rm B}}+\frac{k_aN_0\theta_{\rm B}}{\Omega_1}\right)^{-1}\left(\frac{N_0}{\Omega_7\kappa_5^2}-\frac{N_0}{\Omega_6\kappa_4^2}\right)^{-1}$$
$$\times\left(\left(\frac{N_0}{\Omega_6\kappa_4^2}+\frac{k_aN_0\theta_{\rm B}}{\Omega_1\rho_{\rm B}}+\frac{N_0\theta_{\rm B}}{\Omega_2\rho_{\rm B}}\right)^{-1}-\left(\frac{N_0}{\Omega_7\kappa_5^2}+\frac{k_aN_0\theta_{\rm B}}{\Omega_1\rho_{\rm B}}+\frac{N_0\theta_{\rm B}}{\Omega_2\rho_{\rm B}}\right)^{-1}\right), \tag{28}$$

respectively.

Proof. Setting $m_i=1$, the desired result can be obtained after some simple algebraic manipulations.

4 HD two-way relaying systems

To make a comparative study of the FD two-way relaying system, in this section, we study the performance of HD two-way relaying systems with imperfect self-interference cancellation.

4.1 System model

For the HD mechanism, the entire communication takes place in two time slots. During the first time slot, both nodes A and B transmit to the relay node R, and the signal received at the relay node is given by

$$y_{\rm R}[i]=hx_{\rm A}[i]+gx_{\rm B}[i]+n_{\rm R}[i]. \tag{29}$$

At the second time slot, the relay forwards a scaled version of $y_{\rm R}[i]$, and the signals received at nodes A and B are given by

$$y_{\rm A}[i+1]=\alpha_2hy_{\rm R}[i]+n_{\rm A}[i+1] \text{ and} \tag{30}$$
$$y_{\rm B}[i+1]=\alpha_2gy_{\rm R}[i]+n_{\rm B}[i+1], \tag{31}$$

respectively, where the scaling factor α_2 is defined as

$$\alpha_2^2=\frac{P_r}{|h|^2P_{\rm A}+|g|^2P_{\rm B}+N_0}. \tag{32}$$

Without loss of generality, we focus on the analysis of node A. Substituting (29) into (30), we have

$$y_{\rm A}[i] = h^2\alpha_2 x_{\rm A}[i] + h\alpha_2 g x_{\rm B}[i] + h\alpha_2 n_{\rm R}[i] + n_{\rm A}[i+1]. \tag{33}$$

After performing interference cancellation, the post-processing signal can be written as

$$\hat{y}_{\rm A}[i] = h\alpha_2 g x_{\rm B}[i] + \hat{h}_{\rm A}\hat{x}_{\rm A}[i] + h\alpha_2 n_{\rm R}[i] + n_{\rm A}[i+1]. \tag{34}$$

Hence, the end-to-end SINR $v_{\rm A}$ can be expressed as

$$v_{\rm A} = \frac{\alpha_2^2|h|^2|g|^2P_{\rm B}}{\alpha_2^2|h|^2N_0 + |\hat{h}_{\rm A}|^2\kappa_3^2P_{\rm A} + N_0} \tag{35}$$

$$= \frac{\frac{\rho_{\rm A}|h|^2P_{\rm A}}{|\hat{h}_{\rm A}|^2\kappa_3^2P_{\rm A}+N_0}\frac{|g|^2P_{\rm B}}{N_0}}{\frac{\rho_{\rm A}|h|^2|P_{\rm A}}{|\hat{h}_{\rm A}|^2\kappa_3^2P_{\rm A}+N_0} + \frac{|h|^2P_{\rm A}+|g|^2P_{\rm B}}{N_0} + 1}. \tag{36}$$

Now define $\gamma_6 = \frac{|\hat{h}_{\rm A}|^2\kappa_3^2P_{\rm A}}{N_0} + 1$, and then $v_{\rm A}$ can be rewritten as

$$v_{\rm A} = \frac{\frac{\rho_{\rm A}\gamma_1}{\gamma_6}\gamma_2}{\frac{\rho_{\rm A}\gamma_1}{\gamma_6} + \gamma_1 + \gamma_2 + 1}. \tag{37}$$

Similarly, the received SINR at node B can be expressed as

$$v_{\rm B} = \frac{\frac{\rho_{\rm B}\gamma_2}{\gamma_7}\gamma_1}{\frac{\rho_{\rm B}\gamma_2}{\gamma_7} + \gamma_1 + \gamma_2 + 1}, \tag{38}$$

where $\gamma_7 = \frac{|\hat{h}_{\rm B}|^2\kappa_5^2P_{\rm B}}{N_0} + 1$.

4.2 Performance analysis

Let us assume that nodes A and B are transmitting at constant rates $R_{\rm A}^{\rm HD}$ and $R_{\rm B}^{\rm HD}$, respectively. Let $\eta_{\rm A} = 2^{R_{\rm B}^{\rm HD}} - 1$ and $\eta_{\rm B} = 2^{R_{\rm A}^{\rm HD}} - 1$, and then the outage probabilities at nodes A and B are given by

$$P_{\rm OA}^{\rm H} = \Pr(v_{\rm A} < \eta_{\rm A}) \ \ \text{and} \ \ P_{\rm OB}^{\rm H} = \Pr(v_{\rm B} < \eta_{\rm B}), \tag{39}$$

respectively. Also, the average sum throughput can be computed as

$$\tau_{\rm FD} = R_{\rm B}(1 - P_{\rm OA}^{\rm H}) + R_{\rm A}(1 - P_{\rm OB}^{\rm H}). \tag{40}$$

As in the full-duplex scenario, an exact analysis of the outage probability is challenging. Hence, we look for tractable bounds as presented in the following theorem.

Theorem 2. The outage probability lower bounds at node A $P_{\rm OA}^{\rm HL}$ and node B $P_{\rm OB}^{\rm HL}$ are given by

$$P_{\rm OA}^{\rm HL} = 1 - \frac{\beta_4^{m_4}{\rm e}^{-\frac{\beta_1\eta_{\rm A}+\beta_2\eta_{\rm A}}{\rho_{\rm A}} - \beta_2\eta_{\rm A}}}{\Gamma(m_4)}\sum_{i=0}^{m_1-1}\frac{1}{i!}\left(\frac{\beta_1\eta_{\rm A}}{\rho_{\rm A}}\right)^i\sum_{j=0}^{m_2-1}\frac{1}{j!}\left(\frac{\beta_2\eta_{\rm A}}{\rho_{\rm A}}\right)^j$$
$$\times\sum_{t=0}^{j}\binom{j}{t}\rho_{\rm A}^{j-t}\sum_{p=0}^{t+i}\binom{t+i}{p}\Gamma(p+m_4)\left(\frac{\beta_1\eta_{\rm A}+\beta_2\eta_{\rm A}}{\rho_{\rm A}} + \beta_4\right)^{-p-m_4} \tag{41}$$

and

$$P_{\rm OB}^{\rm HL} = 1 - \frac{\beta_7^{m_7}{\rm e}^{-\frac{(\beta_1\eta_{\rm B}+\beta_2\eta_{\rm B})}{\rho_{\rm B}} - \beta_1\eta_{\rm B}}}{\Gamma(m_7)}\sum_{i=0}^{m_2-1}\frac{1}{i!}\left(\frac{\beta_2\eta_{\rm B}}{\rho_{\rm B}}\right)^i\sum_{j=0}^{m_1-1}\frac{1}{j!}\left(\frac{\beta_1\eta_{\rm B}}{\rho_{\rm B}}\right)^j$$
$$\times\sum_{t=0}^{j}\binom{j}{t}\rho_{\rm B}^{j-t}\sum_{p=0}^{t+i}\binom{t+i}{p}\Gamma(p+m_7)\left(\frac{\beta_1\eta_{\rm B}+\beta_2\eta_{\rm B}}{\rho_{\rm B}} + \beta_7\right)^{-p-m_7}. \tag{42}$$

Proof. See Appendix B.

For the special case with Rayleigh fading, simplified expressions are available as shown in the following corollary.

Corollary 4. For the special case of Rayleigh fading, the outage probability reduces to

$$P_{\rm OA}^{\rm HL} = 1 - \beta_4 {\rm e}^{-\frac{\beta_1\eta_{\rm A}+\beta_2\eta_{\rm A}}{\rho_{\rm A}} - \beta_2\eta_{\rm A}} \left(\frac{\beta_1\eta_{\rm A}+\beta_2\eta_{\rm A}}{\rho_{\rm A}} + \beta_4\right)^{-1} \tag{43}$$

and

$$P_{\rm OB}^{\rm HL} = 1 - \beta_7 {\rm e}^{-\frac{\beta_1\eta_{\rm B}+\beta_2\eta_{\rm B}}{\rho_{\rm B}} - \beta_1\eta_{\rm B}} \left(\frac{\beta_1\eta_{\rm B}+\beta_2\eta_{\rm B}}{\rho_{\rm B}} + \beta_7\right)^{-1}. \tag{44}$$

Proof. Setting $m_i = 1$, the desired result can be obtained after some simple algebraic manipulations.

4.3 Asymptotical analysis

We look into the asymptotic regime, where the transmit powers at all three nodes become large, i.e., $P_{\rm A} \rightarrow \infty$, $P_{\rm B} = k_a P_{\rm A}$, $P_{\rm R} = \rho_{\rm A} P_{\rm A}$.

Proposition 2. In the asymptotic high SNR regime, the outage probability of nodes A and B can be approximated as

$$\begin{aligned} P_{\rm OA}^{\rm HL} \approx & 1 - \frac{1}{\Gamma(m_4)} \left(\frac{m_4 N_0}{\Omega_4 \kappa_3^2}\right)^{m_4} \sum_{i=0}^{m_1-1} \frac{1}{i!} \left(\frac{m_1 N_0 x}{\Omega_1 \rho_{\rm A}}\right)^i \sum_{j=0}^{m_2-1} \frac{1}{j!} \left(\frac{m_2 N_0 x}{\Omega_2 k_a \rho_{\rm A}}\right)^j \\ & \times \Gamma(j+i+m_4) \left(\frac{m_1 N_0 x}{\Omega_1 \rho_{\rm A}} + \frac{m_2 N_0 x}{\Omega_2 k_a \rho_{\rm A}} + \frac{m_4 N_0}{\Omega_4 \kappa_3^2}\right)^{-j-i-m_4} \end{aligned} \tag{45}$$

and

$$\begin{aligned} P_{\rm OB}^{\rm HL} \approx & 1 - \frac{1}{\Gamma(m_7)} \left(\frac{m_7 N_0}{\Omega_7 \kappa_5^2}\right)^{m_7} \sum_{i=0}^{m_2-1} \frac{1}{i!} \left(\frac{m_2 N_0 \eta_{\rm B}}{\Omega_2 \rho_{\rm B}}\right)^i \sum_{j=0}^{m_1-1} \frac{1}{j!} \left(\frac{k_a m_1 N_0 \eta_{\rm B}}{\Omega_1 \rho_{\rm B}}\right)^j \\ & \times \Gamma(j+i+m_7) \left(\frac{k_a m_1 N_0 \eta_{\rm B}}{\Omega_1 \rho_{\rm B}} + \frac{m_2 N_0 \eta_{\rm B}}{\Omega_2 \rho_{\rm B}} + \frac{m_7 N_0}{\Omega_7 \kappa_5^2}\right)^{-j-i-m_7}. \end{aligned} \tag{46}$$

Proposition 2 indicates that the outage probability of the HD two-way relaying system settles in the high SNR regime. This is intuitive because the residual self-interference scales with the transmit power.

Corollary 5. For the special Rayleigh fading, it reduces to

$$P_{\rm OA}^{\rm HL} \approx= 1 - \left(\frac{N_0}{\Omega_4 \kappa_3^2}\right) \left(\frac{N_0 \theta_{\rm A}}{\Omega_1 \rho_{\rm A}} + \frac{N_0 \theta_{\rm A}}{\Omega_2 k_a \rho_{\rm A}} + \frac{N_0}{\Omega_4 \kappa_3^2}\right)^{-1} \tag{47}$$

and

$$P_{\rm OB}^{\rm HL} \approx 1 - \left(\frac{N_0}{\Omega_7 \kappa_5^2 k_a}\right) \left(\frac{N_0 \theta_{\rm B}}{\Omega_1 \rho_{\rm B}} + \frac{N_0 \theta_{\rm B}}{\Omega_2 k_a \rho_{\rm B}} + \frac{N_0}{\Omega_7 \kappa_5^2 k_a}\right)^{-1}. \tag{48}$$

Proof. Setting $m_i = 1$, the desired result can be obtained after some simple algebraic manipulations.

5 Numerical results

In this section, numerical results are presented to verify the analytical expressions derived in Sections 3 and 4, as well as to illustrate the impact of key system parameters on the outage probability and sum throughput performance. Unless otherwise specify, the following set of parameters is used. $m_1 = m_2 = 3$, $m_3 = m_4 = m_5 = m_6 = m_7 = 1$, $\Omega_1 = \Omega_2 = 1$, $\Omega_3 = \Omega_5 = \Omega_6 = 0.5$, $\Omega_4 = \Omega_7 = 0.1$, $\kappa_i = 0.1$, $i = 1, 2, 3, 4, 5$, $\rho_{\rm A} = 2$, $\rho_{\rm B} = 1$, $R_{\rm A}^{\rm FD} = R_{\rm B}^{\rm FD} = 2$ bps/Hz. All the simulation curves are generated by averaging over 10^8 independent trials.

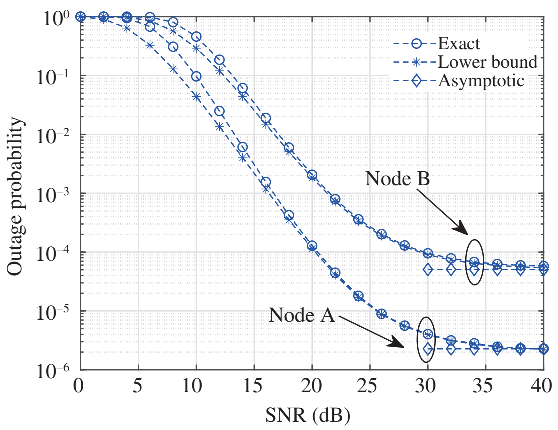

Figure 2 (Color online) Validation of the outage lower bound and asymptotic result.

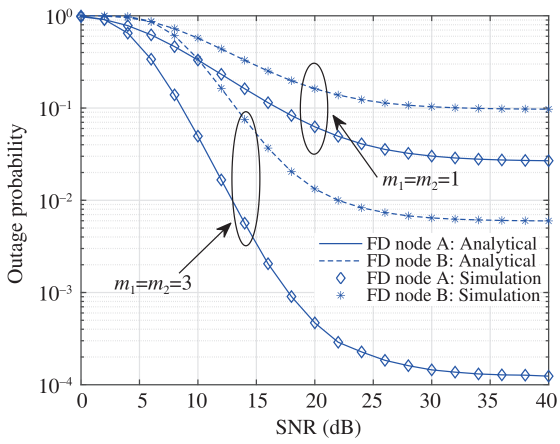

Figure 3 (Color online) Outage probability of nodes A and B.

Figure 2 shows the accuracy of the proposed outage lower bound and asymptotic results. As can be readily observed, the proposed outage lower bound is quite tight, especially in the high SNR regime. Also, the asymptotic results match well with the exact results in the high SNR regime. Moreover, according to simulations, the tightness of the lower bound improves when the level of residual interference reduces.

Figure 3 illustrates the outage performance of the FD two-way relaying systems. The analytical curves are generated as per Theorem 1, and the simulation results are for the outage lower bound. As can be readily observed, the analytical curves overlap with the simulation curves, which validates the correctness of the analytical expressions. In addition, with less severe fading, i.e., larger m, the outage performance significantly improves, which demonstrates the substantial impact of the fading severity parameter m_1 and m_2 on the outage performance. Moreover, the outage probability settles in the high SNR regime owing to interference as predicted by the asymptotic analysis.

Figure 4 depicts the impact of fading parameter m_i on the outage performance of the FD two-way relaying systems with $m_1 = m_2$ and $m_3 = m_4 = m_5 = m_6 = m_7$. We observe that, for $m_1 = 1$, the outage probability increases for both nodes A and B when m_3 varies from 1 to 6. In contrast, for $m = 3$, the outage probability decreases for node A. This interesting phenomenon implies that the impact of fading of the interference channels on the outage performance depends on the fading condition of the information transmission channels. In addition, we observe that increasing the fading parameter of the information channels substantially improves the outage performance, while the change of fading parameters of the interference channels leads to an insignificant variation of the outage behavior, which suggests the overall impact of fading condition of the interference channels on the outage performance is rather insignificant.

Figure 5 shows the achievable sum throughput of the FD two-way relaying systems. We observe that for $\kappa = 0.1$, the maximum sum throughput of 4 bps/Hz can be achieved when $m_1 = m_2 = 3$, while only 3.8 bps/Hz can be achieved when $m_1 = m_2 = 1$. Also, the maximum achievable sum throughput drops substantially for $\kappa = 0.3$. The above phenomena suggest that the fading parameter m and residual interference level parameter κ have a significant impact on the throughput. In particular, the residual interference is the key performance limiting factor, and a less severe fading scenario can help alleviate the detrimental effect of the residual interference.

Figure 6 compares the outage probability of the FD and HD two-way relaying systems when $m_1 = m_2 = 2$, $\Omega_3 = \Omega_5 = \Omega_6 = 0.1$, $\Omega_4 = \Omega_7 = 0.01$. As can be readily observed, with the same constant transmission rate, i.e., $R_{\rm A}^{\rm FD} = R_{\rm A}^{\rm HD}$ and $R_{\rm B}^{\rm FD} = R_{\rm B}^{\rm HD}$, the outage performance of FD and HD two-way relaying systems is close in the low SNR regime, while the outage difference gradually enlarges as the SNR increases, and a substantial performance gap is observed in the high SNR regime. The reason is that, in the low SNR regime, the residual interference is weak, both the FD and HD two-way relaying systems operate in a noise-limited environment and achieve similar outage performance. In contrast, in the high SNR regime, both systems become interference-limited. Owing to the more severe interference level in the FD two-way relaying system, its outage performance deteriorates more substantially.

We also compare the outage performance of FD systems with the HD system with double transmission rate, i.e., $2R_{\rm A}^{\rm FD} = R_{\rm A}^{\rm HD}$ and $2R_{\rm B}^{\rm FD} = R_{\rm B}^{\rm HD}$. In such case, the maximum long-term sum throughput of FD

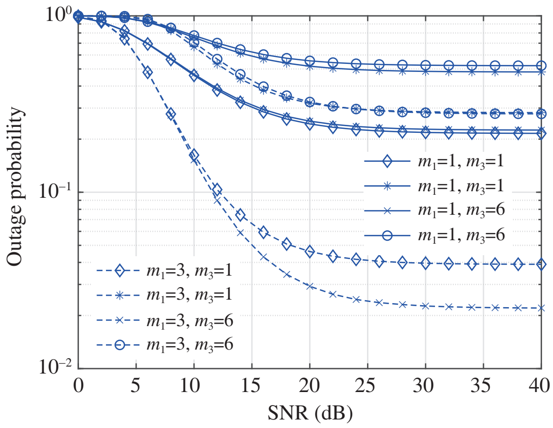

Figure 4 (Color online) Impact of fading parameter m_i on the outage probability.

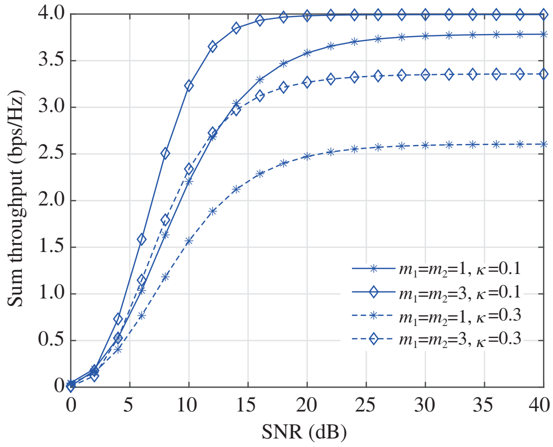

Figure 5 (Color online) Sum throughput of FD two-way relaying systems with different κ and m.

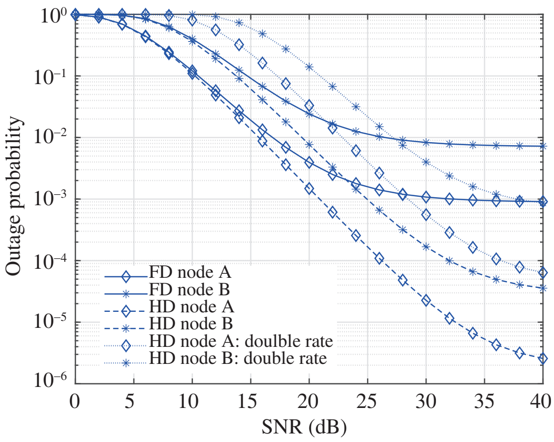

Figure 6 (Color online) Outage probability comparison between FD and HD two-way relaying systems.

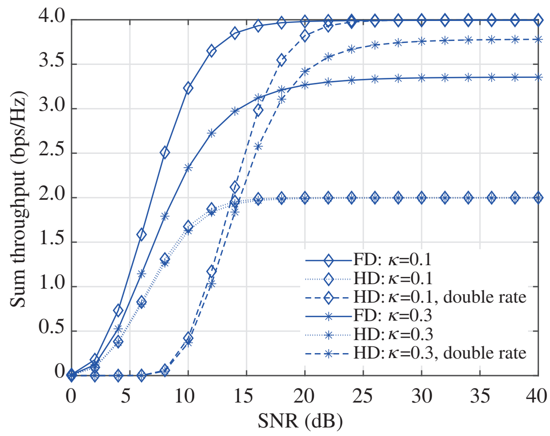

Figure 7 (Color online) Sum throughput comparison between FD and HD two-way relaying systems.

and HD systems becomes identical. We observe that in the low and moderate SNR regime, the outage performance of FD systems is superior to the HD systems. However, in the high SNR regime, the opposite is true, owing to the severe interference in FD systems.

Figure 7 plots the achievable sum throughput of both FD and HD two-way relaying systems. As expected, the FD scheme achieves nearly twice the sum throughput compared with the HD scheme. In addition, we observe that when the residual interference increases, the sum throughput of the FD scheme significantly degrades, while the sum throughput of the HD scheme is almost unaffected. Moreover, when the HD scheme doubles the transmission rate, its effective sum throughput is still inferior to the FD scheme in the low SNR regime. However, when the residual interference is strong, the sum throughput of the HD scheme with a double transmission rate can outperform the FD scheme.

6 Conclusion

This paper has investigated the performance of FD and HD two-way relaying systems. Closed-form expressions have been derived for the outage probability and sum throughput of both FD and HD systems. The analytical results show that the outage probability saturates in the asymptotic high SNR regime, due to the existence of residual interference. In addition, the FD system is not guaranteed to provide superior performance when compared with the HD system. The findings suggest that, given practical constraints on the interference cancellation capability, FD systems shall be deployed in the low and moderate SNR regime. Also, the improvement of the fading condition of the information transmission channels can help mitigate the detrimental effect of residual interference, and thereby significantly enhance the performance of the FD scheme.

Acknowledgements This work was supported by National Key R&D Program of China (Grant No. 2019YFB1803400) and National Natural Science Foundation of China (Grant No. 61922071).

References

1 Wu D, Huang S. Transmission success probability analysis of vehicle users with mobile relays under mobility models. Sci China Inf Sci, 2020, 63: 169304
2 Zhong C J, Jin S, Wong K K. Dual-hop systems with noisy relay and interference-limited destination. IEEE Trans Commun, 2010, 58: 764–768
3 Yang J, Fan P Z, Duong T Q, et al. Exact performance of two-way AF relaying in Nakagami-m fading environment. IEEE Trans Wirel Commun, 2011, 10: 980–987
4 Sabharwal A, Schniter P, Guo D N, et al. In-band full-duplex wireless: challenges and opportunities. IEEE J Sel Areas Commun, 2014, 32: 1637–1652
5 Li X F, Tepedelenlioglu C, Senol H. Channel estimation for residual self-interference in full-duplex amplify-and-forward two-way relays. IEEE Trans Wirel Commun, 2017, 16: 4970–4983
6 Li R Z, Masmoudi A, Le-Ngoc T. Self-interference cancellation with nonlinearity and phase-noise suppression in full-duplex systems. IEEE Trans Veh Technol, 2018, 67: 2118–2129
7 Cheng X L, Yu B, Cheng X, et al. Two-way full-duplex amplify-and-forward relaying. In: Proceedings of IEEE Military Communications Conference, 2013. 1–6
8 Zhang Z Q, Ma Z, Ding Z G, et al. Full-duplex two-way and one-way relaying: average rate, outage probability, and tradeoffs. IEEE Trans Wirel Commun, 2016, 15: 3920–3933
9 Choi D, Lee J H. Outage probability of two-way full-duplex relaying with imperfect channel state information. IEEE Commun Lett, 2014, 18: 933–936
10 Li C, Wang H Y, Yao Y, et al. Outage performance of the full-duplex two-way DF relay system under imperfect CSI. IEEE Access, 2017, 5: 5425–5435
11 Chen H B, Li G, Cai J. Spectral-energy efficiency tradeoff in full-duplex two-way relay networks. IEEE Syst J, 2018, 12: 583–592
12 Cui H Y, Ma M, Song L Y, et al. Relay selection for two-way full duplex relay networks with amplify-and-forward protocol. IEEE Trans Wirel Commun, 2014, 13: 3768–3777
13 Fidan E, Kucur O. Performance of transceiver antenna selection in two way full-duplex relay networks over Rayleigh fading channels. IEEE Trans Veh Technol, 2018, 67: 5909–5921
14 Song K, Li C G, Huang Y M, et al. Antenna selection for two-way full duplex massive MIMO networks with amplify-and-forward relay. Sci China Inf Sci, 2017, 60: 022308
15 Xia B, Li C, Jiang Q M. Outage performance analysis of multi-user selection for two-way full-duplex relay systems. IEEE Commun Lett, 2017, 21: 933–936
16 Li Y, Li N, Peng M G, et al. Relay power control for two-way full-duplex amplify-and-forward relay networks. IEEE Signal Process Lett, 2016, 23: 292–296
17 Koc A, Altunbas A, Yongacoglu A. Outage probability of two-way full-duplex AF relay systems over Nakagami-m fading channels. In: Proceedings of IEEE Vehicular Technology Conference, 2016. 1–5
18 Zhang S, Zhang H, He Q, et al. Joint trajectory and power optimization for UAV relay networks. IEEE Commun Lett, 2018, 22: 161–164
19 Lu Z Y, Sun L L, Zhang S, et al. Optimal power allocation for secure directional modulation networks with a full-duplex UAV user. Sci China Inf Sci, 2019, 62: 080304
20 Bjornson E, Matthaiou M, Debbah M. A new look at Dual-Hop relaying: performance limits with hardware impairments. IEEE Trans Commun, 2013, 61: 4512–4525

Appendix A Proof of Theorem 1

Without loss of generality, we focus on the outage probability at node A. The c.d.f. of $\gamma_{\rm A}^{\rm up}$ can be written as

$$F_{\gamma_{\rm A}^{\rm up}}(x) = \Pr\left(\rho_{\rm A}\min\left(\frac{\gamma_2}{\gamma_3+\rho_{\rm A}\gamma_4}, \frac{\gamma_1}{\gamma_3}\right) \leqslant x\right) \tag{A1}$$

$$= 1 - \Pr\left(\rho_{\rm A}\min\left(\frac{\gamma_2}{\gamma_3+\rho_{\rm A}\gamma_4}, \frac{\gamma_1}{\gamma_3}\right) \geqslant x\right). \tag{A2}$$

Since the two items inside the min function are correlated, it is difficult to handle directly. To circumvent this, we adopt the conditional approach; i.e., we first compute the conditional c.d.f. of $\gamma_{\rm A}^{\rm up}$ by conditioning on γ_3 and γ_4, and then take expectation over γ_3 and γ_4.

Now, conditioned on γ_3 and γ_4, we have

$$F_{\gamma_{\rm A}^{\rm up}}(x|\gamma_3,\gamma_4) = 1 - \Pr\left(\frac{\gamma_2}{\gamma_3+\rho_{\rm A}\gamma_4} \geqslant \frac{x}{\rho_{\rm A}}\middle|\gamma_3,\gamma_4\right)\Pr\left(\frac{\gamma_1}{\gamma_3} \geqslant \frac{x}{\rho_{\rm A}}\middle|\gamma_3,\gamma_4\right). \tag{A3}$$

Since both γ_1 and γ_2 are Gamma distributed, the conditional c.d.f. can be computed as

$$F_{\gamma_{\rm A}^{\rm up}}(x|\gamma_3,\gamma_4) = 1 - \left(1-\gamma\left(m_2, \frac{\beta_2 x(\gamma_3+\rho_{\rm A}\gamma_4)}{\rho_{\rm A}}\right)\right)\left(1-\gamma\left(m_1, \frac{\beta_1\gamma_3 x}{\rho_{\rm A}}\right)\right) \tag{A4}$$

$$= 1 - \left(\sum_{j=0}^{m_2-1}\frac{1}{j!}\left(\frac{\beta_2 x(\gamma_3+\rho_{\rm A}\gamma_4)}{\rho_{\rm A}}\right)^j {\rm e}^{-\frac{\beta_2 x(\gamma_3+\rho_{\rm A}\gamma_4)}{\rho_{\rm A}}}\right)\left(\sum_{i=0}^{m_1-1}\frac{1}{i!}\left(\frac{\beta_1\gamma_3 x}{\rho_{\rm A}}\right)^i {\rm e}^{-\frac{\beta_1\gamma_3 x}{\rho_{\rm A}}}\right), \tag{A5}$$

where $\gamma(n,x)$ is the incomplete Gamma function.

Applying the binomial expansion, and taking expectations over γ_3 and γ_4, we have

$$F_{\gamma_{\rm A}^{\rm up}}(x)=1-\sum_{i=0}^{m_1-1}\frac{1}{i!}\left(\frac{\beta_1 x}{\rho_{\rm A}}\right)^i\sum_{j=0}^{m_2-1}\frac{1}{j!}\left(\frac{\beta_2 x}{\rho_{\rm A}}\right)^j\sum_{k=0}^{j}\binom{j}{k}{\rm E}_{\gamma_3}\left\{\gamma_3^{k+i}{\rm e}^{-\frac{\beta_1 x+\beta_2 x}{\rho_{\rm A}}\gamma_3}\right\}{\rm E}_{\gamma_4}\left\{(\rho_{\rm A}\gamma_4)^{j-k}\,{\rm e}^{-\beta_2 x\gamma_4}\right\}. \tag{A6}$$

To compute ${\rm E}_{\gamma_3}\{\gamma_3^{k+i}{\rm e}^{-\frac{\beta_1 x+\beta_2 x}{\rho_{\rm A}}\gamma_3}\}$, the p.d.f. of random variable γ_3 is required. Utilizing a result[4)], after some algebraic manipulations, it can be shown that the p.d.f. of γ_3 can be obtained as

$$\begin{aligned}f_{\gamma_3}(x)=&\beta_3^{m_3}\beta_4^{m_4}\sum_{s=1}^{m_3}\frac{\prod_{j=1}^{s-1}(1-m_4-j)\,(\beta_4-\beta_3)^{1-m_4-s}}{(m_3-s)!(s-1)!}(x-1)^{m_3-s}{\rm e}^{-\beta_3(x-1)}\\&+\beta_3^{m_3}\beta_4^{m_4}\sum_{s=1}^{m_4}\frac{\prod_{j=1}^{s-1}(1-m_3-j)\,(\beta_3-\beta_4)^{1-m_3-s}}{(m_4-s)!(s-1)!}(x-1)^{m_4-s}{\rm e}^{-\beta_4(x-1)}.\end{aligned}\tag{A7}$$

Hence, we have

$$\begin{aligned}&{\rm E}_{\gamma_3}\left\{\gamma_3^{k+i}{\rm e}^{-\frac{\beta_1 x+\beta_2 x}{\rho_{\rm A}}\gamma_3}\right\}=\beta_3^{m_3}\beta_4^{m_4}{\rm e}^{-\frac{\beta_1 x+\beta_2 x}{\rho_{\rm A}}}\\&\times\left(\sum_{s=1}^{m_3}\frac{\prod_{j=1}^{s-1}(1-m_4-j)\,(\beta_4-\beta_3)^{1-m_4-s}}{(m_3-s)!(s-1)!}\sum_{t=0}^{k+i}\binom{k+i}{t}\left(\beta_3+\frac{\beta_1 x+\beta_2 x}{\rho_{\rm A}}\right)^{-(m_3+t-s+1)}\Gamma(m_3+t-s+1)\right.\\&\left.+\sum_{s=1}^{m_4}\frac{\prod_{j=1}^{s-1}(1-m_3-j)\,(\beta_3-\beta_4)^{1-m_3-s}}{(m_4-s)!(s-1)!}\sum_{t=0}^{k+i}\binom{k+i}{t}\left(\beta_4+\frac{\beta_1 x+\beta_2 x}{\rho_{\rm A}}\right)^{-(m_4+t-s+1)}\Gamma(m_4+t-s+1)\right).\end{aligned}\tag{A8}$$

Finally, the term ${\rm E}_{\gamma_4}\{(\rho_{\rm A}\gamma_4)^{j-k}\,{\rm e}^{-\beta_2 x\gamma_4}\}$ can be computed as

$${\rm E}_{\gamma_4}\left\{(\rho_{\rm A}\gamma_4)^{j-k}\,{\rm e}^{-\beta_2 x\gamma_4}\right\}=\frac{\beta_5^{m_5}}{\Gamma(m_5)}\int_1^\infty(\gamma_4-1)^{m_5-1}{\rm e}^{-\beta_5(\gamma_4-1)}(\rho_{\rm A}\gamma_4)^{j-k}{\rm e}^{-\beta_2 x\gamma_4}{\rm d}\gamma_4 \tag{A9}$$

$$=\frac{\beta_5^{m_5}\rho_{\rm A}^{j-k}{\rm e}^{-\beta_2 x}}{\Gamma(m_5)}\sum_{t=0}^{j-k}\binom{j-k}{t}\int_0^\infty y^{m_5+t-1}{\rm e}^{-(\beta_5+\beta_2 x)y}{\rm d}y \tag{A10}$$

$$=\frac{\beta_5^{m_5}\rho_{\rm A}^{j-k}{\rm e}^{-\beta_2 x}}{\Gamma(m_5)}\sum_{t=0}^{j-k}\binom{j-k}{t}(\beta_5+\beta_2 x)^{-(m_5+t)}\Gamma(m_5+t). \tag{A11}$$

To this end, pulling everything together yields the desired result.

Appendix B Proof of Theorem 2

Following the similar lines as the full-duplex relaying case, the SINRs at nodes A and B can be upper bounded by

$$v_{\rm A}\leqslant v_{\rm A}^{\rm up}=\rho_{\rm A}\min\left(\frac{\gamma_2}{\gamma_6+\rho_{\rm A}},\frac{\gamma_1}{\gamma_6}\right) \tag{B1}$$

and

$$v_{\rm B}\leqslant v_{\rm B}^{\rm up}=\rho_{\rm B}\min\left(\frac{\gamma_1}{\gamma_7+\rho_{\rm B}},\frac{\gamma_2}{\gamma_7}\right). \tag{B2}$$

Without loss of generality, we focus on $P_{\rm OA}^{\rm HL}$. Conditioned on γ_6 and invoking the c.d.f. of γ_1 and γ_2, the outage probability lower bound can be expressed as

$$P_{\rm OA}^{\rm HL}=1-{\rm e}^{-\beta_2\eta_{\rm A}}\sum_{i=0}^{m_1-1}\frac{1}{i!}\left(\frac{\beta_1\eta_{\rm A}}{\rho_{\rm A}}\right)^i\sum_{j=0}^{m_2-1}\frac{1}{j!}\left(\frac{\beta_2\eta_{\rm A}}{\rho_{\rm A}}\right)^j(\gamma_6+\rho_{\rm A})^j\gamma_6^i{\rm e}^{-\frac{(\beta_1\eta_{\rm A}+\beta_2\eta_{\rm A})\gamma_6}{\rho_{\rm A}}}. \tag{B3}$$

Then, taking expectation on γ_6, the outage probability lower bound can be written as

$$\begin{aligned}P_{\rm OA}^{\rm HL}=&1-\frac{\beta_4^{m_4}{\rm e}^{-\beta_2\eta_{\rm A}}}{\Gamma(m_4)}\sum_{i=0}^{m_1-1}\frac{1}{i!}\left(\frac{\beta_1\eta_{\rm A}}{\rho_{\rm A}}\right)^i\sum_{j=0}^{m_2-1}\frac{1}{j!}\left(\frac{\beta_2\eta_{\rm A}}{\rho_{\rm A}}\right)^j\sum_{t=0}^{j}\binom{j}{t}\rho_{\rm A}^{j-t}\\&\times\int_1^\infty\gamma_6^{t+i}{\rm e}^{-\frac{(\beta_1\eta_{\rm A}+\beta_2\eta_{\rm A})\gamma_6}{\rho_{\rm A}}}(\gamma_6-1)^{m_4-1}{\rm e}^{-\beta_4(\gamma_6-1)}d\gamma_6.\end{aligned}\tag{B4}$$

With a change of variable, and then applying the binomial expansion, the above expression can be computed as

$$\begin{aligned}P_{\rm OA}^{\rm HL}=&1-\frac{\beta_4^{m_4}{\rm e}^{-\frac{\beta_1\eta_{\rm A}+\beta_2\eta_{\rm A}}{\rho_{\rm A}}-\beta_2\eta_{\rm A}}}{\Gamma(m_4)}\sum_{i=0}^{m_1-1}\frac{1}{i!}\left(\frac{\beta_1\eta_{\rm A}}{\rho_{\rm A}}\right)^i\sum_{j=0}^{m_2-1}\frac{1}{j!}\left(\frac{\beta_2\eta_{\rm A}}{\rho_{\rm A}}\right)^j\sum_{t=0}^{j}\binom{j}{t}\rho_{\rm A}^{j-t}\\&\times\sum_{p=0}^{t+i}\binom{t+i}{p}\int_0^\infty\gamma_6^{m_4+p-1}{\rm e}^{-\frac{(\beta_1\eta_{\rm A}+\beta_2\eta_{\rm A})\gamma_6}{\rho_{\rm A}}-\beta_4\gamma_6}{\rm d}\gamma_6.\end{aligned}\tag{B5}$$

To this end, the desired result can be obtained by solving the integral.

4) Abu-Dayya A, Beaulieu N. Outage probability of cellular mobile radio systems with multiple Nakagami interferers. IEEE Trans Veh Tech, 1991, 41: 757–768.